

# Generation of Narrow-Band Polarization-Entangled Photon Pairs for Atomic Quantum Memories

Xiao-Hui Bao,<sup>1,2</sup> Yong Qian,<sup>1</sup> Jian Yang,<sup>1</sup> Han Zhang,<sup>1</sup> Zeng-Bing Chen,<sup>1</sup> Tao Yang,<sup>1</sup> and Jian-Wei Pan<sup>1,2</sup>

<sup>1</sup>*Hefei National Laboratory for Physical Sciences at Microscale and Department of Modern Physics, University of Science and Technology of China, Hefei, Anhui 230026, China*

<sup>2</sup>*Physikalisches Institut der Universitaet Heidelberg, Philosophenweg 12, Heidelberg 69120, Germany*  
(Dated: November 6, 2018)

We report an experimental realization of a narrow-band polarization-entangled photon source with a linewidth of 9.6 MHz through cavity-enhanced spontaneous parametric down-conversion. This linewidth is comparable to the typical linewidth of atomic ensemble based quantum memories. Single-mode output is realized by setting a reasonable cavity length difference between different polarizations, using of temperature controlled etalons and actively stabilizing the cavity. The entangled property is characterized with quantum state tomography, giving a fidelity of 94% between our state and a maximally entangled state. The coherence length is directly measured to be 32 m through two-photon interference.

PACS numbers: 03.67.Bg, 42.65.Lm

The storage of photonic entanglement with quantum memories plays an essential role in linear optical quantum computation (LOQC) [1] to efficiently generate large cluster states [2], and in long-distance quantum communication (LDQC) to make efficient entanglement connections between different segments in a quantum repeater [3]. For the atomic ensemble based quantum memories [4, 5, 6], typical spectrum linewidth required for photons is on the order of several MHz. While spontaneous parametric down-conversion (SPDC) is the main method to generate entangled photons [7], the linewidth determined by the phase-matching condition is usually on the order of several THz which is about  $10^6$  times larger, making it unfeasible to be stored. Moreover, interference of independent broad-band SPDC sources requires a synchronization precision of several hundred fs [8]. While in LDQC, for the distance on the order of several hundred km, it becomes extremely challenging for the current synchronization technology [9, 10]. But for a narrow-band continuous-wave source at MHz level, due to the long coherence time, synchronization technique will be unnecessary, while coincidence measurements with time resolution of several ns with current commercial single-photon detectors will be enough to interfere independent sources.

Passive filtering with optical etalons is a direct way to get MHz level narrow-band entangled photons from the broad-band SPDC source, but it will inevitably result in a rather low count rate. In contrast, cavity-enhanced SPDC [11, 12] provides a good solution for this problem. By putting the nonlinear crystal inside a cavity, the generation probability for the down-converted photons whose frequency matches the cavity mode will be enhanced greatly. The cavity acts as an active filter. The frequency of the generated photons lies within the cavity mode, which can be easily set to match the required atomic linewidth. Experimentally, Ou *et al.* [11] has

realized a type-I source, in which the two photons generated have the same polarization, making it very difficult to generate entanglement. Wang *et al.* [13] made a further step by putting two type-I nonlinear crystals within a ring cavity to generate polarization entanglement, but unfortunately the output is multi-mode which does not fit the requirement of an atomic quantum memory. While, a type-II configured source (down-converted photons have different polarizations) is more preferable for the ease of generating polarization entanglement, compared with a type-I source. Recently Kuklewicz *et al.* [14] have realized a type-II source, but the output is still multi-mode. So far to the best of our knowledge, a true narrow-band (single-mode) polarization-entangled photon source at MHz level has never been reported yet along this line. Direct generation of narrow-band photon pairs from cold atomic ensembles [15, 16] is another solution, but the setup is usually much more complicated.

In this Letter, we show that for a type-II cavity-enhanced source by setting a cavity length difference between different polarizations we can reduce the proportion for the background modes greatly. Further suppression is realized by using filter etalons to make the output single-mode. Entanglement is generated by interfering the photon pair on a polarizing beam-splitter (PBS). The measured linewidth for this narrow-band polarization-entangled source is 9.6 MHz, which is comparable to the typical linewidth of atomic quantum memories.

In our experiment, a flux-grown periodically poled KTiOPO<sub>4</sub> (PPKTP) crystal (1cm long) is used as the nonlinear medium. Quasi-phase matching is optimized for a horizontally (H) polarized ultraviolet (UV) pump photon (390 nm) down-converting to a near-infrared photon pair (780 nm) with one polarized in H and the other in vertical (V). The phase-matching bandwidth is 175 GHz. The first side of the PPKTP is high-reflection coated ( $R > 99\%$  at 780 nm) to form the double-resonant

cavity with a concave mirror ( $R \approx 97\%$  at 780 nm) of 10-cm curvature, as shown in FIG. 1. The second side of the PPKTP is anti-reflection (AR) coated to minimize losses within the cavity. Both the PPKTP and the concave mirror are AR coated at 390 nm so that the UV pump interacts only once with the PPKTP in the cavity.

The cavity is intermittently locked using the Pound-Drever-Hall scheme [17]. A mechanical chopper is designed to block the cavity output when the locking beam is switched on, to avoid the leaking beam entering into posterior single-photon detectors. This locking system is only effective for the cavity noise whose frequency is much lower than the locking repetition rate (50 Hz), i.e. the long-term drift. In order to suppress the high frequency noise, especially the strong acoustic noise at subkilohertz, we build the cavity from a single block of stainless steel by digging out the inner part. The PPKTP crystal along with the oven, the thermal electric cooler (TEC) and the concave mirror are fixed firmly inside. The steel block is covered from lateral side with two pieces of organic glass to prevent airflow. Temperature of the PPKTP crystal is controlled to the precision of about 0.002 °C with a high-performance temperature controller. The frequency of the locking beam is the same as the center frequency ( $\omega_0$ ) of the down-converted photons. Since the polarization of the locking beam is rotated to H before entering the cavity, this active locking system can only guarantee the resonance at  $\omega_0$  for H. The resonance of the cavity at  $\omega_0$  for V is realized by slightly tuning the temperature of the PPKTP.

It has been pointed out that for the case of type-II configured cavity-enhanced SPDC, ideally the output will be single-mode [18]. But considering into the finite finesse of the cavity, the ideal single-mode output will be mixed with several nearby background modes. The quantum state can be expressed as:

$$\begin{aligned}
 |\Psi\rangle &= \sqrt{\chi_0}|\omega_0\rangle_H|\omega_0\rangle_V \\
 &+ \sum_{m=1}^{N=46} \frac{\sqrt{\chi_m}}{2} (|\omega_0 + m\Omega_H\rangle_H|\omega_0 - m\Omega_H\rangle_V \\
 &+ |\omega_0 - m\Omega_H\rangle_H|\omega_0 + m\Omega_H\rangle_V \\
 &+ |\omega_0 + m\Omega_V\rangle_H|\omega_0 - m\Omega_V\rangle_V \\
 &+ |\omega_0 - m\Omega_V\rangle_H|\omega_0 + m\Omega_V\rangle_V)
 \end{aligned} \quad (1)$$

with

$$\frac{\chi_m}{\chi_0} = \frac{4}{1 + \frac{4F^2}{\pi^2} \sin^2 \frac{m\Delta\Omega}{\Omega} \pi} \quad (2)$$

where  $\Omega_H$  and  $\Omega_V$  are the free spectrum ranges (FSR) for H and V respectively, with the average value of  $\Omega$  (1.9 GHz) and the difference of  $\Delta\Omega$  (21 MHz);  $F$  is the finesse of the cavity, with the measure value of 166;  $N$  is determined by the phase-matching bandwidth of PPKTP. The first term of the right side of Eq. (1) is the expected single-mode output. The following four terms

in the summation correspond to the case that one photon is resonant with the cavity while the other is not. For the modes near  $\omega_0$ , we have  $\chi_1/\chi_0 = 1.7$ ,  $\chi_2/\chi_0 = 0.63$ ,  $\chi_3/\chi_0 = 0.31$ . When  $m$  goes higher,  $\chi_m$  asymptotically goes to 0. While in the case of equal cavity length ( $\Delta\Omega = 0$ ) [14], each  $\chi_m$  nearly has the same value. The ratio between the summation of these background modes to the center mode is 3.41. In our experiment, we use etalons (FSR = 13.9 GHz, Finesse = 31) to eliminate these nearby modes. The etalons are put into separate copper ovens, and temperature controlled to the precision of 0.01 °C to achieve a stable performance.

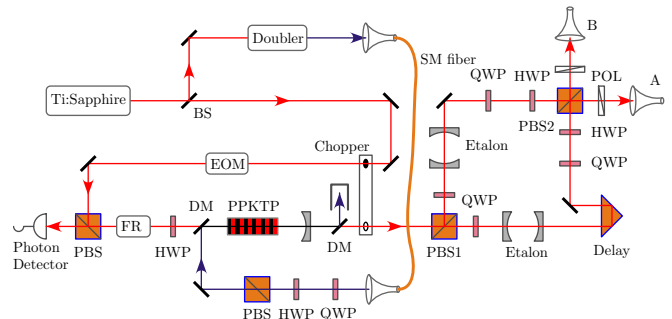


FIG. 1: (color online). Layout of the experiment. The generation of polarization entanglement is realized by interfering the two down-converted photons on PBS2. An electro-optic modulator (EOM) phase modulated at 70 MHz is utilized to generate sidebands for the locking beam. A PBS, a Faraday rotator (FR) and a half-wave plate (HWP) is utilized to extract the reflection beam and to generate the error signal for the locking system.

The complete experimental setup is illustratively shown in FIG. 1. A frequency-stabilized Ti:Sapphire laser with a linewidth of 75 kHz is utilized as the main laser. A small proportion of the output power is split as the locking beam, and the rest power is sent to an eternal-cavity frequency doubler. The generated UV beam is very elliptical, and we use several cylindrical lenses to convert it to a near-Gaussian beam, which is further coupled into a single-mode fiber and released later with a fiber collimator. Two high-performance dichroic mirrors (DM) are used to combine the UV pump with the locking beam, and later separate the remained UV pump from the cavity output. The generated photon pair is separated on PBS1, and filtered with separated etalons. In our experiment we find that slight reflection from the etalons will cause the double-resonant cavity very unstable. We add a quarter-wave plate (QWP) in each path to form an optical isolator with PBS1 to eliminate the etalon reflection.

By making a two-photon interference for the narrow-band photons on PBS2, with one photon polarized in  $|+\rangle = 1/\sqrt{2}(|H\rangle + |V\rangle)$  and the other in  $|-\rangle = 1/\sqrt{2}(|H\rangle - |V\rangle)$  as input, we are able to generate polarization entanglement for the case one photon in each

output port. These two photons are further coupled into single-mode fibers and detected with single-photon detectors. The desired output state is  $|\phi^-\rangle = 1/\sqrt{2}(|H\rangle|H\rangle - |V\rangle|V\rangle)$ . But during the overlapping on PBS2 there is some phase shift between  $|H\rangle$  and  $|V\rangle$ , leading to an output state of  $1/\sqrt{2}(|H\rangle|H\rangle - e^{i\alpha}|V\rangle|V\rangle)$ . We insert an adjustable wave-plate in one output path to compensate this phase shift. In order to verify the entanglement property, we first make a polarization correlation measurement at 4 mW pump power, with the result shown in FIG.2(a). The visibility is about 97%, which is far beyond the requirement for a violation of Bell-CHSH inequality [19]. In this inequality the value  $S$  is defined as

$$S = |E(\phi_A, \phi_B) - E(\phi_A, \phi'_B) + E(\phi'_A, \phi_B) + E(\phi'_A, \phi'_B)| \quad (3)$$

where  $\phi_A$  and  $\phi'_A$  are two polarization measuring angles for photon A, and  $\phi_B$  and  $\phi'_B$  for photon B, and  $E(\alpha, \beta)$  is the correlation coefficient between these two photons. Violation of this inequality ( $S > 2$ ) is a direct proof of entanglement. Our measured result is  $S = 2.66 \pm 0.03$ , for which the inequality is violated by 22 standard deviations. In order to get a more complete characterization of the entanglement, we also make a quantum state tomography [20, 21] for our narrow-band entangled source, the result is shown in FIG.2(b). From the tomography result, the calculated fidelity between our state and  $|\phi^-\rangle$  is 94.3%.

The correlation time between the down-converted photons is inversely proportional to the bandwidth for a SPDC source [22]. Therefore, a narrow-band source at MHz level should exhibit a correlation time which is much longer compared with the broad-band SPDC source (typically on the order of several hundred fs). In our experiment the detector signal of photon A is sent to a time-to-amplitude converter (TAC) as the start signal, and the signal of photon B is used as the stop signal. The TAC output signal is sent to a multi-channel analyzer. The measured result is shown in FIG. 3(a). The data is well agreed with the theoretical expectation with the shape of  $e^{-2\pi\Delta\nu|t|}$  [18]. The best fit shows that the linewidth ( $\Delta\nu$ ) is about 9.6 MHz, which is well within the cavity linewidth. The resolution time of the TAC utilized is about 50 ps, but the single-photon detectors only have a resolution time of 350 ps, which is comparable to the cavity round trip time of 520 ps. Therefore [23], this time correlation measurement can not distinguish our source from previous multi-mode cavity-enhanced SPDC sources. To prove the single-mode property of our source we measure the coherence length directly through the two-photon interference experiment. This is done by observing the polarization correlation visibility in  $|+\rangle/|-\rangle$  basis between photon A and B, as a function of the relative delay before PBS2. The result is shown in FIG. 3(b). We find the coherence length to be  $32 \pm 3$  m, which

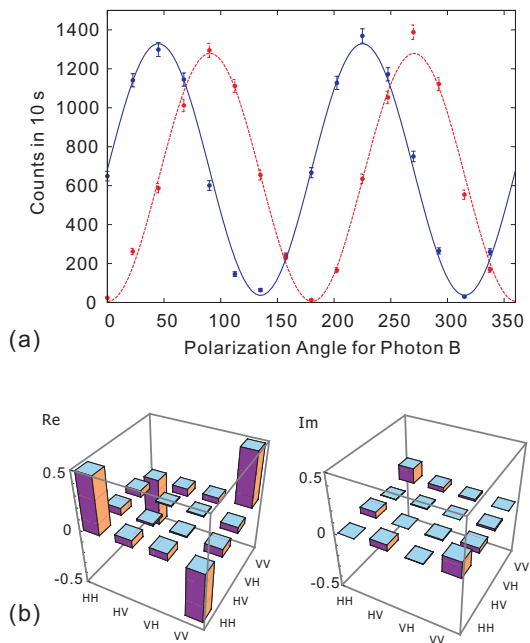


FIG. 2: (color online). (a) Polarization correlations for the entangled photon pair. Polarization angle for photon A is fixed to  $90^\circ$  for the red, and  $-45^\circ$  for the blue. Error bars represent statistical errors. (b) Tomography measurement result, with the left for the real part, the right for the imaginary part.

is consistent with the result from the time correlation measurement in the relation of  $\Delta L = \frac{v}{\Delta\nu}\lambda$ . While for a multi-mode source, determined by the phase-matching condition, the coherence length is usually less than several mm.

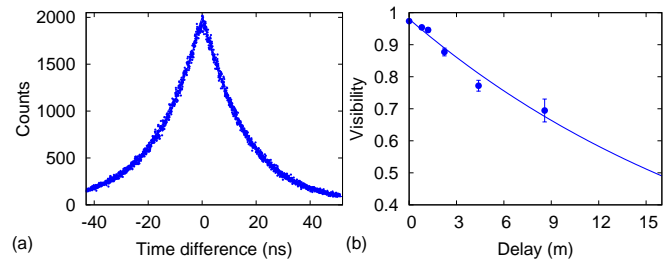


FIG. 3: (color online). (a) Time correlation measurement. The data is fitted with a function of  $c_0 e^{-2\pi\Delta\nu|t|}$ . The FWHM correlation time is 23.0 ns. (b) Visibility in  $|+\rangle/|-\rangle$  basis as a function of the relative delay. The data is fitted with a function of  $v_0 e^{-x/x_0}$ . Error bars represent statistical errors.

For a cavity-enhanced SPDC source, in the case of far below threshold (about 1.88 W for our case), the pair generation rate is proportional to the pump power, which is confirmed by our measured result, which is shown in FIG. 4. At the pump power of 27 mW, we get a maximal pair generation rate of  $1780 \text{ s}^{-1}$  and a corresponding maximal spectrum brightness of  $185 \text{ s}^{-1}\text{MHz}^{-1}$ . We fit the data

with a proportional function and find that the normalized spectrum brightness is about  $6 \text{ s}^{-1}\text{MHz}^{-1}\text{mW}^{-1}$ . Further improvement of the brightness could be possible by employing tighter focus, longer crystal and a cavity with higher finesse.

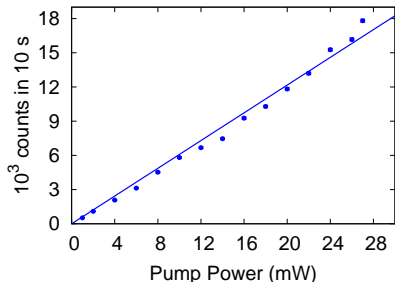


FIG. 4: (color online). Pair generation rate as a function of the UV pump power.

In conclusion, we have experimentally generated narrow-band polarization-entangled photon pairs through cavity-enhanced SPDC with a linewidth of 9.6 MHz, which is comparable to the typical linewidth of atomic quantum memories. Single-mode output is realized by setting a reasonable cavity length difference between different polarizations, using temperature controlled etalons and actively stabilizing the cavity. The wavelength chosen is near Rubidium D2 line, making the storage a straightforward task using the method of electromagnetically induced transparency (EIT) in cold atomic ensembles [5] if the UV pump is set to be pulsed. Since the source is probabilistic and the entanglement is generated through post-selection, one may think that it will limit its applications in LDQC. According to a recent theoretical study [24], both of these problems could be eliminated if applying the same trick. When combined with quantum memories, this narrow-band entangled can be used to efficiently build entanglement over large distance for LDQC, and to efficiently generate large cluster states for LOQC, thus it will have extensive applications in future scalable quantum information

processing.

Thank C.-Z. Peng, B. Zhao and Y.-A. Chen for discussions. This work is supported by the NNSF of China, the CAS, the National Fundamental Research Program (under Grant No. 2006CB921900), and the ERC Grant.

- 
- [1] E. Knill, R. Laflamme and G. J. Milburn, *Nature* **409**, 46 (2001).
  - [2] D. Browne and T. Rudolph, *Phys. Rev. Lett.* **95**, 010501, (2005).
  - [3] H.-J. Briegel, W. Dür, J. I. Cirac and P. Zoller, *Phys. Rev. Lett.* **81**, 5932 (1998).
  - [4] T. Chaneliere *et al.*, *Nature* **438**, 833 (2005).
  - [5] K. Choi, H. Deng, J. Laurat and H. Kimble, *Nature* **452**, 67 (2008).
  - [6] Y.-A. Chen *et al.*, *Nat. Phys.* **4**, 103 (2008).
  - [7] P. G. Kwiat *et al.*, *Phys. Rev. Lett.* **75**, 4337 (1995).
  - [8] M. Zukowski, A. Zeilinger and H. Weinfurter, *Ann. N. Y. Acad. Sci.* **755**, 91 (1995).
  - [9] R. Kaltenbaek *et al.*, *Phys. Rev. Lett.* **96**, 240502 (2006).
  - [10] T. Yang *et al.*, *Phys. Rev. Lett.* **96**, 110501 (2006).
  - [11] Z. Ou and Y. Lu, *Phys. Rev. Lett.* **83**, 2556 (1999).
  - [12] J. Shapiro and N. Wong, *J. Opt. B* **2**, L1 (2000).
  - [13] H. Wang, T. Horikiri and T. Kobayashi, *Phys. Rev. A* **70**, 043804 (2004).
  - [14] C. Kukulicz, F. Wong and J. Shapiro, *Phys. Rev. Lett.* **97**, 223601 (2006).
  - [15] J. Thompson, J. Simon, H. Loh and V. Vuletic, *Science* **313**, 74 (2006).
  - [16] Z.-S. Yuan *et al.*, *Phys. Rev. Lett.* **98**, 180503 (2007).
  - [17] E. Black, *Am. J. Phys.* **69**, 79 (2001).
  - [18] Y. Lu and Z. Ou, *Phys. Rev. A* **62**, 033804 (2000).
  - [19] J. F. Clauser, M. A. Horne, A. Shimony and R. A. Holt, *Phys. Rev. Lett.* **23**, 880 (1969).
  - [20] A. G. White, D. F. V. James, P. H. Eberhard and P. G. Kwiat, *Phys. Rev. Lett.* **83**, 3103 (1999).
  - [21] D. F. V. James, P. G. Kwiat, W. J. Munro and A. G. White, *Phys. Rev. A* **64**, 052312 (2001).
  - [22] C. Hong and L. Mandel, *Phys. Rev. A* **31**, 2409 (1985).
  - [23] H. Goto *et al.*, *Phys. Rev. A* **68**, 015803 (2003).
  - [24] B. Zhao *et al.*, *Phys. Rev. Lett.* **98**, 240502 (2007).